

Original Article

Analysis of Volatile Esters and Alkanoic Acids by an Atmospheric Pressure Corona Discharge Ionization Collision-Induced Dissociation Mass Spectrometry in Positive-Ion Mode: Ionization, Fragmentation Patterns, and Discrimination between Isomeric Compounds

Yuto Nishikido and Kanako Sekimoto*

Graduate School of Nanobioscience, Yokohama City University, 22-2 Seto, Kanazawa-ku, Yokohama, Kanagawa 236-0027, Japan

The ionization and fragmentation patterns of 24 compounds with elemental composition of $C_mH_{2m}O_2$, including isomeric esters and alkanolic acids, were investigated by atmospheric pressure corona discharge ionization collision-induced dissociation (CID) mass spectrometry in the positive-ion mode. All compounds were ionized as protonated molecules and NH_4^+ adducts. In addition, fragment ions were observed in mass spectra of esters other than methyl esters, which are owing to the dissociation of the alkyl group in the alcohol side from the protonated molecules. In CID spectra, protonated alkanolic acids/methyl esters split off H_2O/CH_3OH and CO or the alkyl group in the acid side, depending on the carbon chain length. Protonated esters (other than methyl esters) mainly fragmented the alkyl group in the alcohol side. These general rules on ionization and fragmentation patterns can provide relevant information on the discrimination of isomers.



Copyright © 2023 Yuto Nishikido and Kanako Sekimoto. This is an open-access article distributed under the terms of Creative Commons Attribution Non-Commercial 4.0 International License, which permits use, distribution, and reproduction in any medium, provided the original work is properly cited and is not used for commercial purposes.

Please cite this article as: Mass Spectrom (Tokyo) 2023; 12(1): A0127

Keywords: ester, alkanolic acid, atmospheric pressure corona discharge ionization, fragmentation, positive-ion mode, isomer

(Received April 17, 2023; Accepted: June 26, 2023; advance publication released online July 14, 2023)

1. INTRODUCTION

Fruits biosynthesize and emit a large variety of aroma volatile compounds, and terpenoids and fatty-acid derivatives are the dominant classes. Fruit aroma is an important indicator of the quality of the fruit flavor. For examples, esters are the most abundant volatile compounds emitted by apple, and their use has been proposed for cultivar classification.^{1,2)} Furthermore, it has been reported that watercored (WC) apples have a stronger aroma than non-WC apples because of their relatively high methyl and ethyl esters content; thus, they are widely popular among Japanese consumers.³⁾

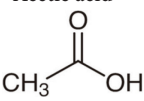
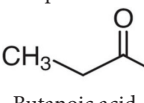
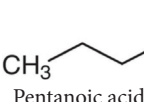
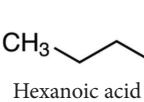
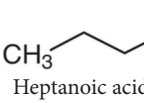
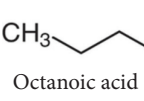
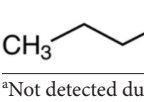
As an important trait of fruit quality, fruit aroma volatile research has gained increasing attention in recent years.⁴⁻¹⁰⁾ The main instrumentation for aroma research used to date are (i) gas chromatography/mass spectrometry (GC/MS)⁵⁻⁸⁾ and (ii) proton-transfer reaction mass spectrometry (PTR-MS).^{9,10)} Comprehensive two-dimensional GC has been used to improve

the separation of different compounds, allowing the separate measurements of hundreds of compounds, including structural and steric isomers. However, the GC technique is time and labor intensive, which limits the number of samples that can be analyzed in practice. Conversely, the PTR-MS, one of the chemical ionization mass spectrometry techniques using H_3O^+ reagent ions, allows the real-time and online measurements of various volatile organic compounds with a high sensitivity and fast response.¹¹⁻¹³⁾ However, the PTR-MS methodology cannot measure isomers separately with the same molecular formulas/mass. Fruit aroma is a complex mixture of a large number of volatile compounds, including isomers. Therefore, the development of real-time measurement techniques that can simultaneously detect various volatile compounds and distinguish isomers would be useful for aroma research in the future.

To achieve this purpose, as a preliminary study, various ester isomers with elemental composition of $C_mH_{2m}O_2$ and

*Correspondence to: Kanako Sekimoto, Graduate School of Nanobioscience, Yokohama City University, 22-2 Seto, Kanazawa-ku, Yokohama, Kanagawa 236-0027, Japan, e-mail: sekimoto@yokohama-cu.ac.jp

Table 1. Summary of seven alkanolic acids ($R_2=H$): the molecular properties and results of positive-ion APCDI mass spectra obtained by the Q-orbitrap MS.

Analyte (M)	Molecular properties				Results of positive-ion APCDI mass spectra: m/z , chemical formula, and relative intensities (%) of major ions					
	Molecular mass (nominal Da)	Formula	R_1	R_2	Protonated molecule, $[M+H]^+$		NH_4^+ adduct, $[M+NH_4]^+$		H_2O loss from protonated molecule, R_1CO^+	
Acetic acid 	60	$C_2H_4O_2$	CH_3	H	61.0283	100	78.0548	71.2	N.D. ^a	
Propanoic acid 	74	$C_3H_6O_2$	C_2H_5	H	75.0439	100	92.0703	24.2	57.0333	3
Butanoic acid 	88	$C_4H_8O_2$	C_3H_7	H	89.0595	100	106.086	31.7	71.049	5
Pentanoic acid 	102	$C_5H_{10}O_2$	C_4H_9	H	103.0751	100	120.1016	18.6	85.0646	3.3
Hexanoic acid 	116	$C_6H_{12}O_2$	C_5H_{11}	H	117.0907	100	134.1171	37.6	99.0802	4.1
Heptanoic acid 	130	$C_7H_{14}O_2$	C_6H_{13}	H	131.1058	100	148.1321	11.3	113.0953	2.5
Octanoic acid 	144	$C_8H_{16}O_2$	C_7H_{15}	H	145.1221	100	162.1486	19.4	127.1116	3.4

^aNot detected due to detection limit of m/z range.

APCDI, atmospheric pressure corona discharge ionization technique; MS, mass spectrometry.

related compounds (e.g., alkanolic acids) are positively ionized by the atmospheric pressure corona discharge ionization technique (APCDI), which is an atmospheric pressure chemical ionization (APCI)-like ambient ionization technique.^{14,15} Thereafter, collision-induced dissociation (CID) is performed for protonated molecules. Resultantly, it is found that those mass spectral data allow distinguishing the isomers. Herein, we discuss general rules on the ionization and fragmentation patterns of alkanolic acid, methyl esters, and other esters. Additionally, we show how the isomers can be distinguished using those rules.

2. EXPERIMENTAL

2.1. Analytes

The analytes used in this study were seven alkanolic acids, seven methyl esters, and ten other esters, as summarized in Tables 1–3. All the analytes were purchased from the Tokyo Chemical Industry (Tokyo, Japan) and had over 98% purity. Hereafter, we use the acronym “ R_1COOR_2 ” to denote

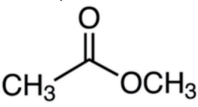
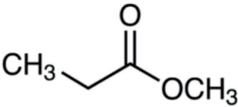
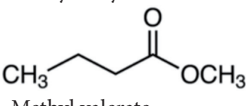
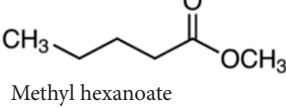
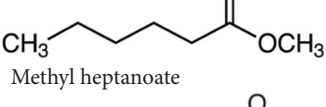
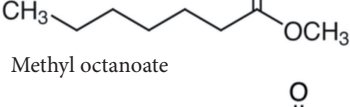
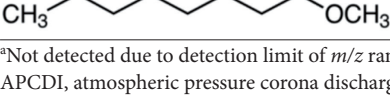
different compounds according to the length of the carbon chain in the acid (R_1) or alcohol side (R_2).

2.2. Atmospheric pressure corona discharge ionization mass spectrometry (APCDI-MS)

Most of the mass spectra were acquired using a Q-Exactive Focus quadrupole-orbitrap mass spectrometer (Thermo Fisher Scientific, Bremen, Germany). The mass resolving power for this instrument was 70,000 at m/z 200 at full width at half maximum, and the measurable m/z was above 50. A TSQ Quantum Discovery MAX triple-quadrupole mass spectrometer (Thermo Fisher Scientific) was used to observe ions below m/z 50. Herein, the two mass spectrometers are abbreviated as “Q-orbitrap MS” and “TQMS.”

The analytes were positively ionized by the well-established APCDI in ambient air with a relative humidity of 50% at 298K, which were controlled using an air conditioner.^{14,15} The corona needle used as the point electrode was a headless stainless steel pin (Shiga, Tokyo, Japan) with a diameter of 200 μ m, 20 mm in length. The needle tip had a radius

Table 2. Summary of seven methyl esters ($R_2=CH_3$): the molecular properties and results of positive-ion APCDI mass spectra obtained by the Q-orbitrap MS.

Analyte (M)	Molecular properties				Results of positive-ion APCDI mass spectra: m/z , chemical formula, and relative intensities (%) of major ions					
	Molecular mass (nominal Da)	Formula	R_1	R_2	Protonated molecule, $[M+H]^+$	NH_4^+ adduct, $[M+NH_4]^+$	CH_3OH loss from protonated molecule, R_1CO^+			
Methyl acetate 	74	$C_3H_6O_2$	CH_3	CH_3	75.0439 $C_3H_7O_2^+$	100 $C_3H_{10}O_2N^+$	92.0703	29.3	N.D. ^a	
Methyl propionate 	89	$C_4H_8O_2$	C_2H_5	CH_3	89.0595 $C_4H_9O_2^+$	100 $C_4H_{12}O_2N^+$	106.086	16.8	57.0334	<1 $C_3H_5O^+$
Methyl butyrate 	102	$C_5H_{10}O_2$	C_3H_7	CH_3	103.075 $C_5H_{11}O_2^+$	100 $C_5H_{14}O_2N^+$	120.102	47.5	71.049	1 $C_4H_7O^+$
Methyl valerate 	116	$C_6H_{12}O_2$	C_4H_9	CH_3	117.091 $C_6H_{13}O_2^+$	100 $C_6H_{16}O_2N^+$	134.117	13.5	85.0648	<1 $C_5H_9O^+$
Methyl hexanoate 	130	$C_7H_{14}O_2$	C_5H_{11}	CH_3	131.106 $C_7H_{15}O_2^+$	100 $C_7H_{18}O_2N^+$	148.132	27.9	99.0804	<1 $C_6H_{11}O^+$
Methyl heptanoate 	144	$C_8H_{16}O_2$	C_6H_{13}	CH_3	145.121 $C_8H_{17}O_2^+$	100 $C_8H_{20}O_2N^+$	162.148	11.6	113.096	<1 $C_7H_{13}O^+$
Methyl octanoate 	158	$C_9H_{18}O_2$	C_7H_{15}	CH_3	159.138 $C_9H_{19}O_2^+$	100 $C_9H_{22}O_2N^+$	176.164	76.7	127.112	<1 $C_8H_{15}O^+$

^aNot detected due to detection limit of m/z range.

APCDI, atmospheric pressure corona discharge ionization technique; MS, mass spectrometry.

of curvature of *ca.* 1 μm , and the shape of the needle tip surface was adequately approximated by a hyperboloid of revolution. The opposite electrode was the stainless steel orifice plate of the mass spectrometers. A positive corona discharge was generated by applying +3.7 kV between the point-to-plane electrodes with 3 mm gap. An Eppendorf microtube (1.5 mL) with each analyte was placed between the needle and the orifice plate. Analytes were diffused into the discharge region and were protonated with hydronium ion H_3O^+ and its water clusters $H_3O^+(H_2O)_n$, which were produced as the major atmospheric background ions in APCDI. This protonation mechanism was analogous to the APCI-like ambient ionization technique, such as direct analysis in real time.¹⁶⁾

In the CID experiments, the width for the selected precursor ions for the Q-orbitrap MS and TQMS was *ca.* ± 0.4 Da and ± 1 Da, respectively. The target gas was N_2 for the Q-Orbitrap MS and Ar for the TQMS. The collision energies in the laboratory were 10–20 eV for both the instruments. In

use of 10 eV, ion dissociation was observed at approximately the minimum energies.

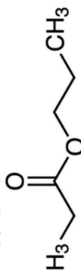
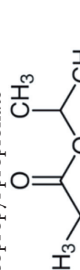
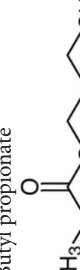



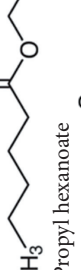
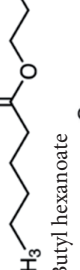
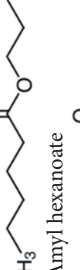
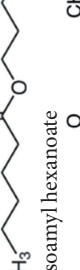
3. RESULTS AND DISCUSSION

3.1. Ionization and fragmentation patterns

3.1.1. Alkanoic acids

Table 1 summarizes the major ions and corresponding intensities detected in the positive-ion APCDI mass spectra of seven alkanolic acids (R_1COOH ; $R_1=C_{1-7}H_{3-15}$). Individual analytes were detected dominantly as protonated molecules $[R_1COOH+H]^+$ and NH_4^+ adducts $[R_1COOH+NH_4]^+$. In using the APCI-like (*i.e.*, plasma-based) ambient ionization technique, ammonium ion, NH_4^+ , can be easily formed as the background ion from air constituents and can attach to heteroatoms in analyte molecules.¹⁷⁾ Notably, H_2O loss from the protonated molecules, $[R_1COOH+H-H_2O]^+$, was observed at a significantly low intensity ($\leq 5\%$ relative to the protonated molecules, as shown in Table 1). For the PTR-MS, relatively

Table 3. Summary of 10 esters other than methyl ester ($R_2 \neq CH_3$): molecular properties and results of positive-ion APCDI mass spectra obtained by the Q-orbitrap MS.

Molecular properties		Results of positive-ion APCDI mass spectra: m/z , chemical formula, and relative intensities (%) of major ions									
Analyte (M)	Molecular mass (nominal Da)	Formula	R_1	R_2	Protonated molecule, $[M+H]^+$	NH_4^+ adduct, $[M+NH_4]^+$	$[R_2-H]$ loss from protonated molecule, $[R_1COOH+H]^+$	R_1 -COOH loss from protonated molecule, R_2^+			
Propyl propanoate 	116	$C_6H_{12}O_2$	C_2H_5	C_3H_7	117.0909 $C_6H_{13}O_2^+$	134.117 $C_6H_{16}O_2N^+$	75.0441 $C_3H_7O_2^+$	29.8	N.D. ^a		
Isopropyl propanoate 	116	$C_6H_{12}O_2$	C_2H_5	C_3H_7	117.0909 $C_6H_{13}O_2^+$	134.117 $C_6H_{16}O_2N^+$	75.0441 $C_3H_7O_2^+$	60.3	N.D. ^a		
Butyl propanoate 	130	$C_7H_{14}O_2$	C_2H_5	C_4H_9	131.1066 $C_7H_{15}O_2^+$	148.133 $C_7H_{18}O_2N^+$	75.044 $C_3H_7O_2^+$	28.5	57.0698 $C_4H_9^+$		
Isobutyl propanoate 	130	$C_7H_{14}O_2$	C_2H_5	C_4H_9	131.1066 $C_7H_{15}O_2^+$	148.133 $C_7H_{18}O_2N^+$	75.044 $C_3H_7O_2^+$	15.4	57.0698 $C_4H_9^+$		
Hexyl acetate 	144	$C_8H_{16}O_2$	CH_3	C_6H_{13}	145.1218 $C_8H_{17}O_2^+$	162.148 $C_8H_{20}O_2N^+$	61.0282 $C_2H_5O_2^+$	17.1	85.1009 $C_6H_{13}^+$		
Ethyl hexanoate 	144	$C_8H_{16}O_2$	C_5H_{11}	C_2H_5	145.1218 $C_8H_{17}O_2^+$	162.148 $C_8H_{20}O_2N^+$	117.091 $C_6H_{13}O_2^+$	14.1	N.D. ^a		
Propyl hexanoate 	158	$C_9H_{18}O_2$	C_5H_{11}	C_3H_7	159.1374 $C_9H_{19}O_2^+$	176.164 $C_9H_{22}O_2N^+$	117.091 $C_6H_{13}O_2^+$	48.6	N.D. ^a		
Butyl hexanoate 	172	$C_{10}H_{20}O_2$	C_5H_{11}	C_4H_9	173.153 $C_{10}H_{21}O_2^+$	190.179 $C_{10}H_{24}O_2N^+$	117.091 $C_6H_{13}O_2^+$	66.5	57.0698 $C_4H_9^+$		
Amyl hexanoate 	186	$C_{11}H_{22}O_2$	C_5H_{11}	C_5H_{11}	187.1686 $C_{11}H_{23}O_2^+$	204.1951 $C_{11}H_{26}O_2N^+$	117.0906 $C_6H_{13}O_2^+$	51.4	71.0853 $C_5H_{11}^+$		
Isoamyl hexanoate 	186	$C_{11}H_{22}O_2$	C_5H_{11}	C_5H_{11}	187.1686 $C_{11}H_{23}O_2^+$	204.1951 $C_{11}H_{26}O_2N^+$	117.0906 $C_6H_{13}O_2^+$	20.6	71.0853 $C_5H_{11}^+$		

^aNot detected due to detection limit of m/z range. APCDI, atmospheric pressure corona discharge ionization technique; MS, mass spectrometry.

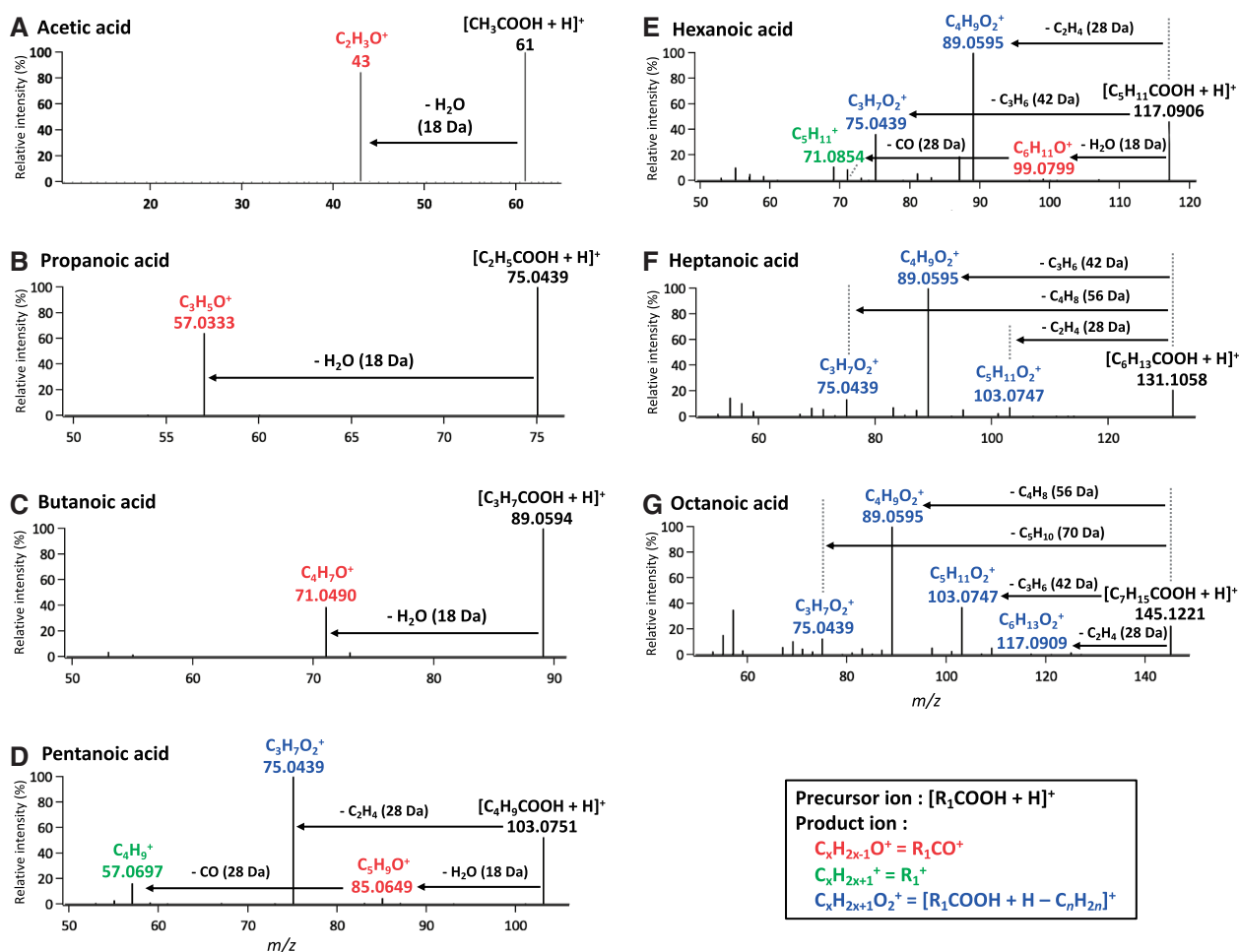


Fig. 1. CID spectra of protonated molecules for seven alkanolic acids ($R_1\text{COOH}$) obtained at a collision energy of 10 eV; (a) acetic acid, (b) propanoic acid, (c) butanoic acid, (d) pentanoic acid, (e) hexanoic acid, (f) heptanoic acid, and (g) octanoic acid. All the spectra other than those of acetic acid (A) were acquired by the Q-orbitrap MS, whereas acetic acid spectra were obtained by the triple-quadrupole mass spectrometer. Mass spectral data for ion species with relative intensities higher than 1.5% are summarized in Table S1. CID, collision-induced dissociation; MS, mass spectrometry. The spectrum data files are available in J-STAGE Data. <https://doi.org/10.50893/data.massspectrometry.23591499>

high intensities of H_2O loss were observed (92%, 47%, 32%, 34%, and 60% from the protonated molecules of the alkanolic acids with $R_1=\text{CH}_3$, C_2H_5 , C_3H_7 , C_4H_9 , and C_5H_{11} , respectively).¹⁸⁾ This indicates that the APCDI-MS is a softer ionization technique than the PTR-MS.

The CID experiments were performed for the protonated molecules $[\text{R}_1\text{COOH}+\text{H}]^+$. The CID spectra obtained at a collision energy of 10 eV are shown in Fig. 1. The fragmentation patterns varied depending on the carbon chain length of R_1 . When the carbon chain was short ($R_1=\text{C}_{1-3}\text{H}_{3-7}$), H_2O loss was dominant to form acylium ion, R_1CO^+ (product ions in red color in Fig. 1a–1c). Furthermore, CO was lost from the R_1CO^+ ion with R_1 larger than C_3H_7 (product ions in green color in Fig. S1a in the Supplementary Information and Fig. 1d and 1e). For the relatively long carbon chain ($R_1=\text{C}_{4-7}\text{H}_{9-15}$), the loss of C_nH_{2n} ($n\geq 2$), originating from a part of the alkyl group in R_1 , became more dominant than the loss of $\text{H}_2\text{O}+\text{CO}$. The resulting product ions, $[\text{R}_1\text{COOH}+\text{H}-\text{C}_n\text{H}_{2n}]^+$ (blue color in Fig. 1d–1g) have the same chemical structure as the protonated molecules of relatively small alkanolic acids. For example, the product ions at m/z 89 (assigned as $\text{C}_4\text{H}_9\text{O}_2^+$) observed in the CID spectra for $[\text{C}_{4-7}\text{H}_{9-15}\text{COOH}+\text{H}]^+$ (Fig. 1d–1g) corresponded with protonated butanoic acid. This is evidenced

by the similarity of the CID spectral patterns between the $\text{C}_4\text{H}_9\text{O}_2^+$ at m/z 89 originating from $[\text{C}_{5-7}\text{H}_{11-15}\text{COOH}+\text{H}]^+$ (which were obtained in combination with in-source CID, as shown in Fig. S2a) and the protonated butanoic acid (Fig. 1c). Among the product ions $[\text{R}_1\text{COOH}+\text{H}-\text{C}_n\text{H}_{2n}]^+$ observed from various precursor ions, $\text{C}_4\text{H}_9\text{O}_2^+$ at m/z 89 (*i.e.*, protonated butanoic acid) was dominant, thereby indicating its significant stability.

With increasing collision energies, fragmentation proceeded, resulting in higher intensities of product ions formed from secondary dissociation. As an example, CID spectra of protonated pentanoic acid $[\text{C}_4\text{H}_9\text{COOH}+\text{H}]^+$ obtained at collision energies of 15 and 20 eV are shown in Fig. S3a.

3.1.2. Methyl esters

The ionization and fragmentation patterns for methyl esters were considerably similar to those for the alkanolic acids described earlier. The methyl esters (R_1COOCH_3) were ionized as protonated molecules, $[\text{R}_1\text{COOCH}_3+\text{H}]^+$, and NH_4^+ adducts, $[\text{R}_1\text{COOCH}_3+\text{NH}_4]^+$ (Table 2). The dominant fragmentation pattern of the $[\text{R}_1\text{COOCH}_3+\text{H}]^+$ ions with relatively short carbon chains of R_1 ($R_1=\text{C}_{1-4}\text{H}_{3-9}$) was the loss of CH_3OH to form the acylium ion, R_1CO^+ (red color in

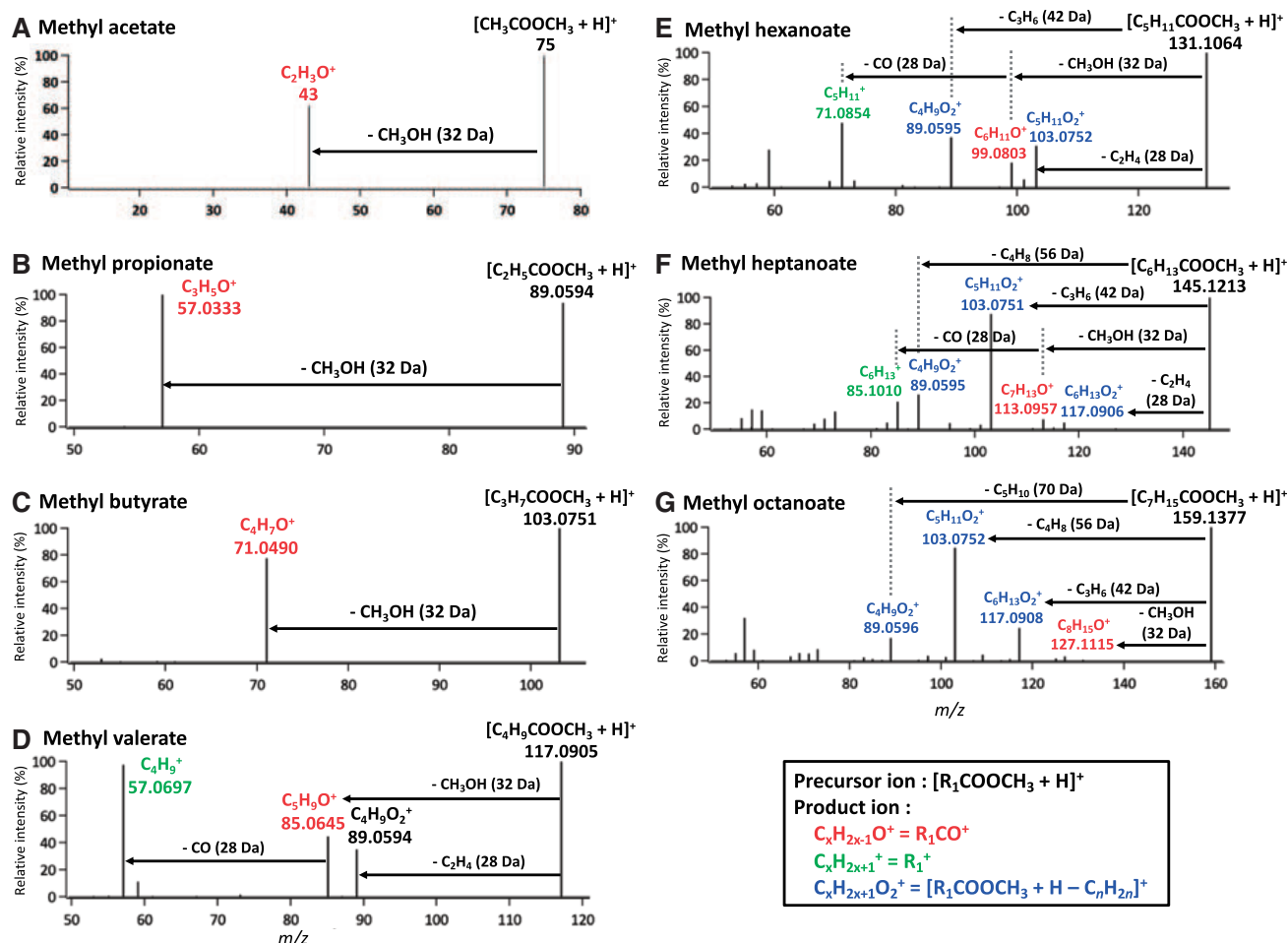


Fig. 2. CID spectra of protonated molecules for seven methyl esters (R_1COOCH_3) obtained at a collision energy of 10 eV; (a) methyl acetate, (b) methyl propionate, (c) methyl butyrate, (d) methyl valerate, (e) methyl hexanoate, (f) methyl heptanoate, and (g) methyl octanoate. All the spectra other than those of methyl acetate (A) were acquired by the Q-orbitrap MS, whereas the methyl acetate spectra were obtained by the triple-quadrupole mass spectrometer. Mass spectral data for ion species with relative intensities higher than 1.5% are summarized in Table S1. CID, collision-induced dissociation; MS, mass spectrometry. The spectrum data files are available in J-STAGE Data. <https://doi.org/10.50893/data.massspectrometry.23591574>

Fig. 2a–2d). Furthermore, as the carbon chain became longer, CO loss occurred successively (product ions in green color in Fig. S1b in the Supplementary information and Fig. 2d). For protonated methyl hexanoate ($\text{R}_1=\text{C}_5\text{H}_{11}$) with middle length of carbon chain, the loss of alkyl fragments, C_nH_{2n} , from R_1 ($n \geq 2$), as well as $\text{CH}_3\text{OH}+\text{CO}$, was observed (product ions in blue vs. red+green color in Fig. 2e). Protonated methyl esters with relatively long carbon chains ($\text{R}_1=\text{C}_{6,7}\text{H}_{13,15}$) dominantly dissociated C_nH_{2n} to form product ions $[\text{R}_1\text{COOCH}_3+\text{H}-\text{C}_n\text{H}_{2n}]^+$, as compared with the loss of $\text{CH}_3\text{OH}+\text{CO}$ (Fig. 2f and 2g). The product ions $[\text{R}_1\text{COOCH}_3+\text{H}-\text{C}_n\text{H}_{2n}]^+$ were identical to the protonated molecules of relatively small methyl esters, evidenced by the similarity of their CID spectral patterns (Fig. S2b). Higher collision energies progressed fragmentation in which intensities of product ions formed by secondary dissociation were increased (see CID spectra of protonated methyl valerate $[\text{C}_4\text{H}_9\text{COOCH}_3+\text{H}]^+$ obtained at collision energies of 15 and 20 eV shown in Fig. S3b).

3.1.3. Esters other than methyl ester

Esters other than methyl esters (R_1COOR_2 ; $\text{R}_2 \neq \text{H}, \text{CH}_3$) were ionized as protonated molecules $[\text{R}_1\text{COOR}_2+\text{H}]^+$ and NH_4^+ adducts $[\text{R}_1\text{COOR}_2+\text{NH}_4]^+$ as with the alkanolic

acids and methyl esters (Table 3). Additionally, fragment ions due to the dissociation of $[\text{R}_2-\text{H}]$ or R_2COOH from the protonated molecules, *i.e.*, $[\text{R}_1\text{COOH}+\text{H}]^+$ or R_2^+ , were observed with relatively high intensities (Table 3). Those fragment ions originated from McLafferty rearrangement¹⁹ and are dominant product ions in the CID spectra of the protonated molecules (red and blue colors in Fig. 3). Furthermore, secondary dissociation from the product ions $[\text{R}_1\text{COOH}+\text{H}]^+$ was observed (product ions in yellow color in Fig. 3), with similar CID patterns of the protonated alkanolic acids, as shown in Fig. 1. If the proton transfers to the fragment $[\text{R}_2-\text{H}]$, the product ion R_2^+ is detected. Higher collision energies resulted in progress of secondary dissociation (see CID spectra of protonated propyl propionate $[\text{C}_2\text{H}_5\text{COOC}_3\text{H}_7+\text{H}]^+$ obtained at collision energies of 15 and 20 eV shown in Fig. S3c).

Notably, in the CID spectra obtained here, the intensities of the precursor ions at the lowest collision energy of 10 eV were considerably low (approximately zero) for all the esters. These results suggest that the protonated esters ($\text{R}_2 \neq \text{H}, \text{CH}_3$) can easily dissociate the R_2 part to form the protonated alkanolic acids including the R_1 part, which is independent of the carbon chain length of R_2 .

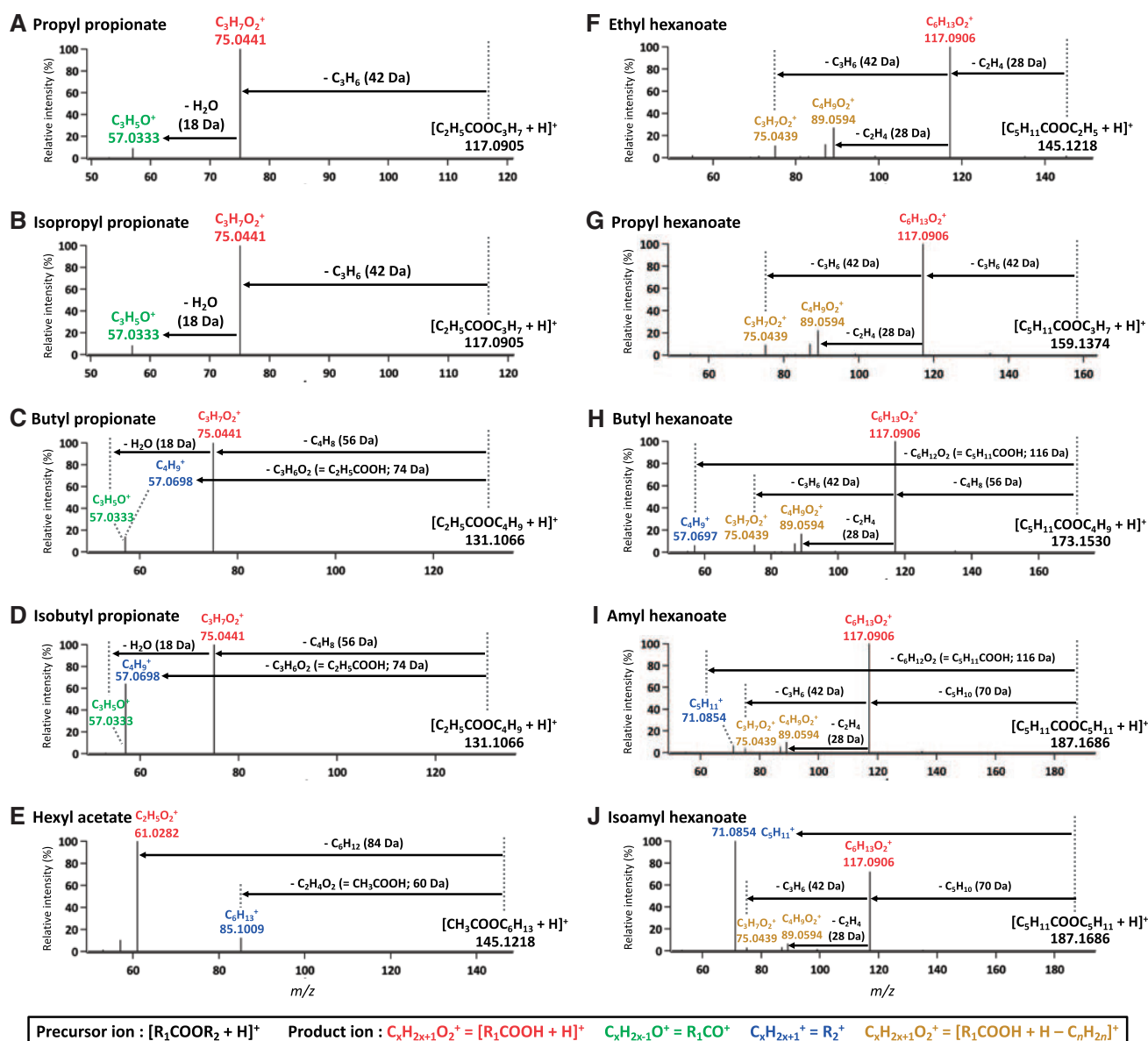


Fig. 3. CID spectra of protonated molecules for ten esters other than methyl esters (R_1COOR_2 ; $R_2 \neq H, CH_3$) obtained at a collision energy of 10 eV; (a) propyl propionate, (b) isopropyl propionate, (c) butyl propionate, (d) isobutyl propionate, (e) hexyl acetate, (f) ethyl hexanoate, (g) propyl hexanoate, (h) butyl hexanoate, (i) amyl hexanoate, and (j) isoamyl hexanoate. The secondary dissociation from product ions $C_xH_{2x+1}O_2^+$ (in red color) was confirmed by CID with in-source CID (Fig. S2c). Mass spectral data for ion species with relative intensities higher than 1.5% are summarized in Table S1. CID, collision-induced dissociation; MS, mass spectrometry. The spectrum data files are available in J-STAGE Data. <https://doi.org/10.50893/data.massspectrometry.23591583>

3.2. Discrimination of isomeric compounds

The systematic ionization and fragmentation patterns described earlier allow us to distinguish the isomeric compounds of alkanolic acids, methyl esters, and other esters. First, suppose that a protonated molecule and NH_4^+ adduct of an unknown $C_mH_{2m}O_2$ with an m number less than or equal to 3 ($m \leq 3$) is detected in a mass spectrum. If the CID of the protonated molecule $[C_mH_{2m}O_2 + H]^+$ leads to the detection of a product ion resulting from the loss of H_2O or CH_3OH , $C_mH_{2m}O_2$ can be identified as an alkanolic acid or methyl ester; if neither H_2O nor CH_3OH is lost, $C_mH_{2m}O_2$ should be esters other than methyl ester.

Next, suppose that an unknown $C_mH_{2m}O_2$ has an m number greater than 4 ($m \geq 4$). If the CID of its protonated molecule generates product ions resulting from CH_3OH loss, the

$C_mH_{2m}O_2$ is determined as a methyl ester; no loss of CH_3OH indicates other ester or alkanolic acid. $C_mH_{2m}O_2$ can be distinguished as an ester or an alkanolic acid by determining the intensity of the precursor ion $[C_mH_{2m}O_2 + H]^+$ in the CID spectrum. If the relative intensity of $[C_mH_{2m}O_2 + H]^+$ is considerably low (<5%), $C_mH_{2m}O_2$ should be an ester. Differences in precursor ion intensity are clearly seen when the collision energy is low such as 10 eV. Therefore, it is preferable to use low collision energy for discrimination of isomers focused in this study.

If there is only the protonated molecule of $C_mH_{2m}O_2$ (not NH_4^+ adduct), the $[C_mH_{2m}O_2 + H]^+$ should be a fragment from the protonated molecule of esters other than methyl esters. In this case, we should check whether $[C_mH_{2m}O_2 + H]^+$ and $[C_mH_{2m}O_2 + NH_4]^+$ originating from esters are in high m/z regions.

4. CONCLUSIONS

This study provided some basic data on isomeric esters and alkanolic acids with elemental composition of $C_mH_{2m}O_2$ measured by APCDI-CID-MS in the positive-ion mode. We explained that there are general rules for the ionization and fragmentation patterns of protonated molecules for those compounds, which makes it possible to distinguish the isomers. These rules should enable the development of real-time measurement techniques that can detect various compounds simultaneously but distinguish isomers; furthermore, they will contribute to aroma research in the future.

ACKNOWLEDGMENT

This work was supported by JSPS KAKENHI grant numbers JP21K19111, JP21K12223, and JP23H04969.

REFERENCES

- 1) D. Holland, O. Larkov, I. Bar-Yaakov, E. Bar, A. Zax, E. Brandeis, U. Ravid, E. Lewinsohn. Developmental and varietal differences in volatile ester formation and acetyl-CoA: Alcohol acetyl transferase activities in apple (*Malus domestica* Borkh.) fruit. *J. Agric. Food Chem.* 53: 7198–7203, 2005.
- 2) R. G. Berger. Flavours and Fragrances – Chemistry, Bioprocessing and Sustainability; Springer-Verlag, Berlin, Germany, 2007.
- 3) F. Tanaka, K. Okazaki, T. Kashimura, Y. Ohwaki, M. Tatsuki, A. Sawada, T. Ito, T. Miyazawa. Profiles and physiological mechanisms of sensory attributes and flavor components in watercored apple. *Nippon Shokuhin Kagaku Kogaku Kaishi* 63: 101–116, 2016 (in Japanese).
- 4) M. A. M. El Hadi, F.-J. Zhang, F.-E. Wu, C.-H. Zhou, J. Tao. Advances in fruit aroma volatile research. *Molecules* 18: 8200–8229, 2013.
- 5) C. B. Steingass, R. Carle, H.-G. Schmarr. Ripening-dependent metabolic changes in the volatiles of pineapple (*Ananas comosus* (L.) Merr.) fruit: I. Characterization of pineapple aroma compounds by comprehensive two-dimensional gas chromatography-mass spectrometry. *Anal. Bioanal. Chem.* 407: 2591–2608, 2015.
- 6) C. B. Steingass, M. Jutzi, J. Muller, R. Carle, H.-G. Schmarr. Ripening-dependent metabolic changes in the volatiles of pineapple (*Ananas comosus* (L.) Merr.) fruit: II. Multivariate statistical profiling of pineapple aroma compounds based on comprehensive two-dimensional gas chromatography-mass spectrometry. *Anal. Bioanal. Chem.* 407: 2609–2624, 2015.
- 7) A. Muto, C. T. Muller, L. Bruno, L. McGregor, A. Ferrante, A. A. C. Chiappetta, M. B. Bitonti, H. J. Rogers, N. D. Spadafora. Fruit volatilome profiling through GC × GC-TOF-MS and gene expression analyses reveal differences amongst peach cultivars in their response to cold storage. *Sci. Rep.* 10: 18333, 2020.
- 8) X. Song, L. Zhu, X. Geng, Q. Li, F. Zheng, Q. Zhao, J. Ji, J. Sun, H. Li, J. Wu, M. Zhao, B. Sun. Analysis, occurrence, and potential sensory significance of tropical fruit aroma thiols, 3-mercaptohexanol and 4-methyl-4-mercapto-2-pentanone, in Chinese Baijiu. *Food Chem.* 363: 130232, 2021.
- 9) F. Ciesa, I. Höller, W. Guerra, J. Berger, J. Dalla Via, M. Oberhuber. Chemodiversity in the fingerprint analysis of volatile organic compounds (VOCs) of 35 old and 7 modern apple cultivars determined by proton-transfer-reaction mass spectrometry (PTR-MS) in two different seasons. *Chem. Biodivers.* 12: 800–812, 2015.
- 10) T. Bianchi, Y. Weesepeel, A. Koot, I. Iglesias, I. Eduardo, M. Gratacos-Cubarsi, L. Guerrero, M. Hortos, S. van Ruth. Investigation of the aroma of commercial peach (*Prunus persica* L. Batsch) types by proton transfer reaction-mass spectrometry (PTR-MS) and sensory analysis. *Food Res. Int.* 99: 133–146, 2017.
- 11) W. Lindinger, A. Hansel, A. Jordan. On-line monitoring of volatile organic compounds at PPTV levels by means of proton-transfer-reaction mass spectrometry (PTR-MS) medical applications, food control and environmental research. *Int. J. Mass Spectrom. Ion Process.* 173: 191–241, 1998.
- 12) B. Yuan, A. R. Koss, C. Warneke, M. Coggon, K. Sekimoto, J. de Gouw. Proton-transfer-reaction mass spectrometry: Applications in atmospheric sciences. *Chem. Rev.* 117: 13187–13229, 2017.
- 13) K. Sekimoto, A. R. Koss. Modern mass spectrometry in atmospheric sciences: Measurement of volatile organic compounds in the troposphere using proton-transfer-reaction mass spectrometry. *J. Mass Spectrom.* 56: e4619, 2021.
- 14) K. Sekimoto, M. Takayama. Negative ion formation and evolution in atmospheric pressure corona discharges between point-to-plane electrodes with arbitrary needle angle. *Eur. Phys. J. D* 60: 589–599, 2010.
- 15) K. Sekimoto, M. Sakai, M. Takayama. Specific interaction between negative atmospheric ions and organic compounds in atmospheric pressure corona discharge ionization mass spectrometry. *J. Am. Soc. Mass Spectrom.* 23: 1109–1119, 2012.
- 16) R. B. Cody, J. A. Laramee, H. D. Durst. Versatile new ion source for the analysis of materials in open air under ambient conditions. *Anal. Chem.* 77: 2297–2302, 2005.
- 17) T. Zhang, W. Zhou, W. Jin, J. Zhou, E. Handberg, Z. Zhu, H. Chen, Q. Jin. Direct desorption/ionization of analytes by microwave plasma torch for ambient mass spectrometric analysis. *J. Mass Spectrom.* 48: 669–676, 2013.
- 18) E. von Hartungen, A. Wisthaler, T. Mikoviny, D. Jaksch, E. Boscaini, P. J. Dunphy, T. D. Märk. Proton-transfer-reaction mass spectrometry (PTR-MS) of carboxylic acids: Determination of Henry's law constants and axillary odour investigations. *Int. J. Mass Spectrom.* 239: 243–248, 2004.
- 19) E. Aprea, F. Biasioli, T. D. Märk, F. Gasperi. PTR-MS study of esters in water and water/ethanol solutions: Fragmentation patterns and partition coefficients. *Int. J. Mass Spectrom.* 262: 114–121, 2007.